Role of the fluidity of a liquid phase in determining the surface properties of the opposite phase at the liquid-liquid interface

Júlia Kertész,[a] Mária Darvas,[b] Pál Jedlovszky,[c,d,e] and George Horvai[a,c,*]

[a]*Department of Inorganic and Analytical Chemistry, Budapest University of Technology and Economics, Szt. Gellért tér 4, H-1111 Budapest, Hungary*

[b]*SISSA, Department of Biological and Statistical Physics, 265 via Bonomea, Trieste, Italy*

[c]*HAS Research Group of Technical Analytical Chemistry, Szt. Gellért tér 4, H-1111 Budapest, Hungary*

[d]*Laboratory of Interfaces and Nanosize Systems, Institute of Chemistry, Eötvös Loránd University, Pázmány Péter stny. 1/a, H-1117 Budapest, Hungary*

[e]*EKF Department of Chemistry, Leányka u. 6, H-3300 Eger, Hungary*

Keywords: Liquid-liquid interface, ITIM analysis, intrinsic surface

Running title: Opposite phase fluidity

[*]**Electronic mail:** george.horvai@mail.bme.hu

Abstract:

Molecular dynamics simulations of the water-CCl_4 interface have been done in two different ways. In the first simulation the CCl_4 phase has been frozen in an equilibrium configuration, and only the water molecules have been allowed to move, whilst in the other one no such artificial freezing has been done. This way the effect of the fluid-like structure and fluid-like dynamics of the CCl_4 phase on the surface properties of the aqueous phase could be investigated separately. Due to the separate thermostatting of the two types of molecules in the simulations all the differences seen between the interfacial properties of water in the two systems can indeed be attributed to the rigid vs. fluid nature of the organic phase, and not to the thermal contact with a phase of zero temperature. The obtained results reveal that the rigidity of the opposite phase introduces an ordering both in the layering structure and orientation of the surface water molecules. The enhanced orientational ordering leads to a stronger lateral hydrogen bonding structure of the molecules within the subsequent molecular layers beneath the surface, and hence also to a slower exchange of the water molecules between the surface and the bulk aqueous phase.

1. Introduction

Investigation of the molecular level properties of various fluid (i.e., liquid-vapour and liquid-liquid) interfaces became the focus of intensive scientific research in the past fifteen years. Although fluid interfaces play a key role in a number of processes of fundamental scientific interest, in living systems, and in numerous industrial applications, such investigations were previously largely prevented by the lack of suitable experimental methods that can selectively probe interfacial molecules. The recent development and spread of this kind of methods, such as nonlinear (e.g., sum frequency generation or second harmonic generation) spectroscopies [1,2] or x-ray and neutron reflectivity measurements [3] enabled scientists to meaningfully address such problems, and thus resulted in a rapidly growing number of such studies [4-24].

Experimental investigations can be well complemented by computer simulation studies, since simulation methods can provide us with a three dimensional model of atomistic resolution of the system of interest. Thus simulations can offer deeper insight into the appropriately chosen model of the system than conventional experiments are likely to reach [25]. The rapid development of the routinely available computing power has led to a significant increase in the number and quality of simulation studies of fluid interfaces [26-55], which has paralleled the similar development in the experimental fields in the past two decades.

However, when simulating fluid interfaces at atomistic resolution one has to face the problem that finding the exact location of the interface in such systems is not a trivial task at all. The problem originates from the fact that fluid interfaces are corrugated by capillary waves due to the thermal motion of the molecules. The task of finding the real, capillary wave-corrugated intrinsic interface is analogous with that of finding the full list of molecules that are located right at the surface of their phase (i.e., in contact with the opposite phase) at every instant along the simulated trajectory. Until recently, the majority of the interfacial simulation studies simply neglected this problem, and used the (ideally planar) Gibbs dividing surface instead of the real, capillary wave-corrugated intrinsic interface. However, it is now clear that this neglect leads to systematic error in the calculated structural properties

[47,56] and composition [44,45,50] of the interface, and even in the thermodynamic properties of the system studied [51]. Thus, for instance, the critical mixing line of the water-benzene system was found to appear at 100-200 K lower temperature than its real location when the interface between the two phases is treated in a non-intrinsic way. [51]. Further, when comparing simulation results with experimental data it is essential to calculate the quantities of interest exactly on the same set of molecules that are probed in the experiment, i.e., the molecules that are located at the real, intrinsic surface of their phase.

The first method designed to determine the intrinsic surface of a fluid phase, proposed by Chacón and Tarazona [57] was followed in the past decade by several alternative approaches, [40,41,56,58-60] some of which do not even require the interface to be macroscopically planar [58,60]. Among these methods the Identification of the Truly Interfacial Molecules (ITIM) [56] has turned out to be an excellent compromise between computational cost and accuracy [59]. In an ITIM analysis the molecules located at the boundary of their phase are detected by moving a probe sphere of a given radius along a large set of test lines from the bulk opposite phase; and the molecules of the phase of interest that are first touched by the probe sphere along any of the test lines are marked as being interfacial [56]. The ITIM method has successfully been applied recently to a set of liquid-liquid [43,46,47,51] and liquid-vapour [44,45,48-50,52-55] interfacial systems. The use of an intrinsic surface analysis method, such as ITIM has the additional advantage that various surface properties, such as intrinsic density [41,42,57,60,61] or free energy profiles [62,63], roughness of the intrinsic surface [49,53,56] and its relation with the surface tension [64], lateral percolation of the surface molecules [51,55,56], dynamics of exchange of the molecules between the surface layer and the bulk phase [43-50,53,65], adsorption of molecules at the surface and its extent in terms of molecular layers [44,45,50], or immersion of large surface molecules (e.g., surfactants) into the bulk phase [65-67] can be meaningfully addressed this way.

In this paper we address another fundamental question, namely the role of the fluidity of one phase in determining the surface properties of the other one at the liquid-liquid interface. At a liquid-liquid interface two dynamically fluctuating fluid phases meet. It is reasonable to assume that some coupling exists between these fluctuations of the phases. It is natural to ask then how would one of the two liquid phases behave if the fluctuations of the

other one were stopped. To address this question we performed molecular dynamics simulations of the water-CCl_4 system in two ways. In the first simulation the molecules of the organic phase were frozen in an equilibrium configuration of the liquid-liquid system, and only the water molecules were allowed to move. This way, the CCl_4 phase was turned into a glass-like phase, and hence it could not adapt to the fluctuations occurring at the surface of the aqueous phase, neither could the capillary waves of CCl_4 exhibit any interference with those of the aqueous surface. In the other simulation, used here for reference, no such artificial freezing has been done, and hence the real water-CCl_4 interface has been simulated. It should be emphasized that the first simulation is not intended to, and does not correspond to any physically relevant system. Computer simulation provides a unique opportunity to formally decouple several factors that cannot be done in real systems, making it possible to analyze their role separately from each other. Our approach takes advantage of this opportunity, by decoupling the fluid-like structure and dynamics of the organic phase in order to analyze their separate roles in determining the properties of the surface of the aqueous phase. The properties of the water surface obtained in the two ways are then compared in terms of density profiles of the subsequent subsurface layers, surface roughness, dynamics of exchange of the bulk phase and surface molecules, as well as orientation and percolation of the surface molecules.

The paper is organized as follows. In Section 2 details of the simulations performed are given. The obtained results are discussed in detail in Section 3. Finally, in Section 4 the main conclusions of this study are summarized.

2. Computational details

Molecular dynamics simulations of the water-CCl_4 liquid-liquid interface have been performed on the isothermal-isobaric (N,p,T) ensemble at 298 K and 1 bar. The rectangular basic simulation box consisted of 4000 water and 2000 CCl_4 molecules. The Y and Z edges of the basic box, being parallel with the macroscopic interface have been set to be 50 Å long, whilst the X axis has been left to fluctuate according to the semi-isotropic pressure coupling applied.

Water and CCl_4 molecules have been described by the rigid TIP4P [68] and OPLS [69] potential models, respectively. According to these models, the total potential energy of the system has been calculated as the sum of the pair interaction energy terms, the latter being equal to the sum of the Lennard-Jones and Coulomb contributions of all the pairs of the interaction sites of the two molecules. The geometry of the water and CCl_4 molecules have been kept unchanged by means of the SETTLE [70] and LINCS [71] algorithms, respectively. All interactions have been truncated to zero beyond the cut-off distance of the molecule centres of 12.5 Å; the long range part of the electrostatic interaction has been taken into account using the Ewald summation method in its smooth particle mesh (PME) implementation [72].

Simulations have been performed using the GROMACS simulation package [73]. The temperature and pressure of the system have been controlled by the Nosé-Hoover [74,75] and Parinello-Rahman [76] algorithms, respectively. The equations of motion have been solved in time steps of 2 fs. Initial configurations have been taken from an earlier simulation of us, thus, even the starting configurations supposed to be in equilibrium [43]. Nevertheless, we further equilibrated the system for 5 ns, during which energetic and structural properties did not change tendentiously. After this eauilibration, two simulations have been performed. In the first of these simulations, referred to here as I or the “frozen” simulation, the CCl_4 molecules have been fixed at their initial positions, and only the water molecules have been moved. Technically this has been done by setting the temperature of the CCl_4 phase to zero. However, since the water and CCl_4 molecules have been thermostatted separately, this treatment has not lead to a cooling down of the aqueous phase (i.e., slowing down of the water molecules) at all. In other words, the separate thermostatting has introduced a perfect virtual non-interacting thermal insulator between the two phases. In the other run, called as II or the “reference” simulation CCl_4 molecules have also been moved in the regular manner, according to the forces acting on them. In both cases a 5 ns long trajectory has been simulated, along which 2500 sample configurations per system, separated by 2 ps long trajectories each, have been saved for further evaluation. The calculated interfacial properties have been averaged for the 2500 sample configurations, including both liquid-liquid interfaces present in the basic simulation box.

The intrinsic surface of the aqueous phase has been identified by means of the ITIM method [56]. In the ITIM analyses a probe sphere of the radius of 1.25 Å has been used, according to the suggestion of Jorge et al. [59]. The test lines along which the probe was moved have been arranged in a 100 × 100 grid across the interfacial plane *YZ*. This resolution corresponds to a distance of 0.5 Å of two neighbouring grid lines, which is sufficient to get an accurate mapping of the water surface [59]. The ITIM procedure has been repeated three times by disregarding the set of molecules identified in the previous steps. This way, the first three molecular layers beneath the surface of the aqueous phase have been identified separately [56]. An instantaneous equilibrium snapshot of the two systems simulated as well as that of the first three subsurface molecular layers of the aqueous phase are shown in Figure 1, as taken from the simulations.

3. Results and discussion

3.1. Density profiles

The mass density profiles of water across the two systems simulated are shown and compared in Figure 2. In addition, the mass density profiles of the first three molecular layers of the aqueous phase are also shown for both systems. As is seen, the rigid opposite phase introduces a certain ordering of the water molecules next to the interface. This ordering is already seen in the overall, non-intrinsic density profile. Namely, unlike in the reference system, the total water mass density profile is not monotonous in system I, when water is in contact with a rigid disordered phase. Thus, in system I the water mass density profile shows three separate maxima of decreasing amplitude upon going away from the interface. This shape of the density profile is typical at liquid-solid interfaces [77-82]. However, in such studies the surface of the solid phase is usually assumed to be ideally flat. On the other hand, intrinsic density profiles obtained at liquid-liquid interfaces also show separate maxima and minima [41,42,57,60,61]. Our present result indicates that the monotonous behaviour of the global, non-intrinsic density profiles obtained at liquid-liquid interfaces [26-39] is the consequence of both the non-intrinsic treatment in the analysis and the fluidity of the opposite phase. Clearly, if any of these two conditions is not satisfied the density profile turns out to be structured. It should be emphasized that while the first of these conditions,

i.e., the non-intrinsic treatment results in an artificial, erroneous smoothing of the density profile, the fluid nature of the opposite phase is a fully physical constraint.

It is also seen from Fig. 2 that the consecutive molecular layers of the aqueous phase become thinner and denser if the opposite phase is rigid (as the corresponding distributions are narrower and higher here than in the reference system). The density profiles of the individual layers can be well fitted by a Gaussian function [83], as seen also from Fig. 2. The position and width parameters of these fitted Gaussians, denoted as X_c and σ, respectively, are collected in Table 1 and can be used as estimates of the position and width of the corresponding molecular layer. As is seen, these layers get 15-25% narrower if the opposite phase becomes rigid, and this difference gradually decreases upon going farther from the interface. Although the positions of the consecutive layers do not differ much in the two systems, a clear trend is seen in the distance of two consecutive layers, namely that in the case of the rigid opposite phase two consecutive water layers are roughly 0.1 Å, i.e., about 3% closer than in the reference case.

3.2. Surface roughness

The determination of the full list of the interfacial molecules provides a unique opportunity also to characterize the molecular scale roughness of the surface of a fluid phase [56]. However, it is clear that the information on the roughness of a wavy surface cannot be condensed into one single parameter. Instead, surface roughness should be characterized by at least two independent parameters, i.e., an amplitude-like and a frequency-like one. Recently we proposed the use of the following parameter pair [49]. The average normal distance $\overline{d}$ of two surface points (i.e., their distance along the macroscopic surface normal axis *X*) exhibits a saturation curve as a function of their lateral (i.e., *YZ*) distance, *l*. (The positions of the surface points are represented here by the positions of the O atoms of the surface water molecules.) The $\overline{d}(l)$ data follow the Langmuir-like function [64]

$$\overline{d} = \frac{a\xi l}{a + \xi l}, \tag{1}$$

where a and ξ are the amplitude-like and frequency-like roughness parameters, respectively.

Here we calculated the $\bar{d}(l)$ data corresponding to the first three consecutive molecular layers of the aqueous phase in both systems simulated. The obtained data together with their fit to Eq. (1) are shown in Figure 3, while the a and ξ parameters are collected in Table 1. As is seen, the amplitude of the consecutive molecular layers of the aqueous phase is decreased by about 25%, whilst their frequency increased by 5-25% upon freezing the opposite phase. The observed decrease of the amplitude parameter is in a clear accordance with the thinning of the subsurface layers, as discussed in the previous sub-section.

3.3. Dynamics of exchange between the surface and the bulk phase

The dynamics of exchange of the molecules between the surface layer and the bulk phase can be characterized by the survival probability of the molecules at the surface, $L(t)$. The survival probability is simply the probability that a molecule which belongs to the surface layer at t_0 remains uninterruptedly there up to $t_0 + t$. Since leaving the surface is a process of first order kinetics, the $L(t)$ survival probability is of exponential decay, and hence the mean residence time of a molecule in the surface layer, τ, can simply be determined by fitting the $\exp(-t/\tau)$ function to the simulated $L(t)$ data.

The $L(t)$ survival probability functions are shown in Figure 4 as obtained in the two systems simulated, whereas the corresponding τ mean residence time values are included in Table 1. As is clear, the freezing of the opposite phase considerably slows down the exchange of the water molecules between the surface and the bulk aqueous phase. Thus, the mean residence time value of the surface water molecules increased by about a factor of two upon freezing the opposite phase. In interpreting this result it should be emphasized once more that, due to the separate thermostatting of the water and CCl_4 molecules, the freezing of the organic phase did not cool down the aqueous phase, i.e., it did not slow down, on average, the water molecules, even if they were in contact with it. Therefore, the observed slowdown of the exchange of molecules between the surface and bulk aqueous phase is indeed a real effect of the rigidity of the opposite phase, as water molecules have the same average velocity in both cases.

3.4. Orientation of the surface molecules

The full characterization of the orientational statistics of rigid molecules relative to an external vector requires the bivariate joint distribution of two independent orientational variables. As we have demonstrated previously, the angular polar coordinates ϑ and ϕ of the external vector (in our case, the macroscopic surface normal vector, $\underline{X}$, pointing, by our convention, towards the apolar phase) in a local Cartesian frame fixed to the individual molecules are suitable orientational parameters for this purpose [84,85]. The local frame fixed to a surface water molecule is defined here in the usual way (see, e.g., Fig. 6 of Ref. 43). Its origin is the O atom, axis *x* is the molecular normal, axis *z* is the symmetry axis of the molecule, oriented in such a way that the *z* coordinates of the H atoms are positive, and axis *y* is perpendicular to the above two. Thus, ϑ is the angle of axis *z* and the macroscopic surface normal vector, $\underline{X}$, while ϕ is the angle between the molecular normal axis *x* and the projection of $\underline{X}$ to the plane perpendicular to the symmetry axis of the water molecule. The molecular axis *x* is oriented in such a way that the relation $0^o \leq \phi \leq 90^o$ holds. Since ϑ is an angle of two general spatial vectors, and ϕ is the angle between two vectors restricted to lay in a given plane (i.e., the *xy* plane of the molecular frame) by definition, uncorrelated orientation of the molecules with the surface results in uniform bivariate distribution only if $\cos\vartheta$ and ϕ are chosen to be the orientational variables [84,85].

Since the orientation of the surface molecules can largely depend on the local curvature of the surface portion they are located at [43,56,80], we have calculated the $P(\cos\vartheta,\phi)$ bivariate orientational distributions not only in the entire surface layer, but also in its three separate regions A, B and C. These regions are defined as follows. Regions A and C cover the *X* ranges where the density of the surface layer is less than half of its maximum value, ρ_{max}, region A being at the organic, whilst region C at the aqueous side of the surface layer. Thus, regions A and C typically cover the crests and troughs, i.e., surface portions of locally convex and concave curvature, respectively, of the molecularly rough liquid surface. Finally, region B is located between regions A and C. The definition of these three separate regions of the surface layer is illustrated in the inset of Fig. 2.

The $P(\cos\vartheta,\phi)$ bivariate orientational distributions are shown in Figure 5 as obtained in the entire surface layer as well as in its separate regions A, B and C of both systems simulated. As is seen, the orientational behaviour of the surface water molecules is qualitatively similar in the two systems. Thus, the water molecules in the entire surface layer prefer to lie parallel to the macroscopic surface plane, *YZ*, as seen from the peak at $\cos\vartheta = 0$ and $\phi = 0^{o}$. Further, this peak extends deeply towards larger ϕ and smaller $\cos\vartheta$ values. A similar picture is obtained in the most populated region, B. Different orientational preferences are seen, however, in regions A and C. In both of these regions a dual orientational preference is found. Instead of lying parallel with the macroscopic surface plane, *YZ*, the water molecules prefer a somewhat tilted alignment in both of these regions. This tilt is such that the two H atoms prefer to point towards the aqueous phase in region A and towards the apolar phase in region C. These orientational preferences are reflected in the peaks of the $P(\cos\vartheta,\phi)$ maps around $\cos\vartheta = \pm 0.3$ and $\phi = 0^{o}$. In the other preferred alignment the water molecule is perpendicular to the macroscopic surface plane, *YZ*, and points by one of its O-H bonds straight towards the apolar phase in region A, and towards the aqueous phase in region C. This preference is evidenced by the peaks at $\cos\vartheta = \pm 0.3$ and $\phi = 90^{o}$. As it has been discussed several times [43,46,47,51,56], these orientational preferences are dictated by the requirement of maximizing the number of hydrogen bonds a surface molecule can form with its neighbours.

Besides the qualitative similarity, however, there is a clear difference between the orientational maps obtained in the two systems. Thus, the maps corresponding to the "frozen" system show noticeably stronger orientational ordering (i.e., higher peaks and more pronounced minima between them) than those of the reference system. In other words, the preferred orientations are the same in the two systems, but the strength of these preferences increases when the opposite phase becomes rigid. This finding also reveals that, besides the increase of the layering order (i.e., smoother, thinner and denser layers) at the interface, the rigidity of the opposite phase increases also the orientational order of the surface molecules of the fluid phase it is in contact with.

3.5. Surface percolation

The water molecules that form the surface layer of a neat aqueous phase at a liquid-vapour or liquid-liquid interface are known to form an infinite lateral, two dimensional percolation network at room temperature [43,46,47,51,55,56], and this network breaks down only about 200 K below the temperature at which the boundary between the two phases disappears [51,55]. It is also known that in the subsurface layers beneath the first molecular layer no such percolation network exists [43,46,47,56].

To investigate the role of the rigidity of the opposite phase on the surface percolation, we have calculated the size distribution of the hydrogen bonded water clusters in the first and second layers of both systems simulated. Two water molecules belonging to the same subsurface molecular layer are regarded as being hydrogen bonded to each other if the distance of their O atoms is less than 3.3 Å, and their shortest intermolecular O···H distance is less than 2.45 Å. These cut-off distances correspond to the first minimum positions of the O-O and O-H radial distribution functions of the used water model. Two water molecules belong to the same hydrogen bonded lateral cluster if they are connected by an intact chain of hydrogen bonded water pairs within the subsurface layer they belong to. The size n of a lateral cluster is simply the number of water molecules that belong to it. In percolating two dimensional systems the $P(n)$ distribution exceeds the critical line of

$$P(n) \sim n^{-2.05} \tag{2}$$

at large cluster size values, whereas in non-percolating systems $P(n)$ drops below this critical line at small or intermediate cluster sizes and remains below that in the entire range of n [86].

The $P(n)$ distributions of the first and second molecular layers of systems I and II are shown and compared in Figure 6. Again, the two systems show qualitatively similar behaviour, as the molecules form a strongly percolating network in the first layer, but do not percolate in the second layer in both cases. However, besides the qualitative similarity there is again a clear difference between the two systems in this respect. Thus, in system I the entire $P(n)$ distribution is shifted to larger n values in both layers than in system II. Thus, the curve corresponding to the first layer of the frozen system clearly exceeds that of the

reference system in the region of its peak around the *n* value of 300, whilst in the case of the second layer, apart from the *n* value of 1, the curve of system I goes above that of system II in the entire *n* range.

This finding indicates that, besides the stronger layering and orientational structure and slower exchange of the molecules between the surface and the bulk phase, a rigid opposite phase leads also to an enhanced hydrogen bonding structure (i.e., more hydrogen bonds per water molecule), at least within a given subsurface molecular layer, compared to the situation when a fluid phase is in contact with the aqueous phase.

4. Summary and conclusions

In this paper we have analysed the subtle differences in the interfacial properties of neat water being in contact with a fluid and a frozen disordered phase. The frozen CCl_4 phase considered is an artificial construction, as its interface with room temperature water does not correspond to any physical system. We have chosen to study this system because of our purely theoretical approach of separating the effect of the fluid-like molecular structure and fluid-like dynamics of the opposite phase on the aqueous phase at the liquid-liquid interface. This separation of the effects of the structural and dynamical properties of the opposite phase can be achieved by "switching off" its dynamics in a molecular dynamics computer simulation. It should be emphasized that although this freezing of the CCl_4 phase is technically achieved by setting its temperature to zero, the separate thermostatting of the water and CCl_4 molecules in the simulation introduces a perfect virtual thermal insulator between the two phases. Therefore, the observed changes in the interfacial properties of the aqueous phase are indeed related to the rigid *versus* fluid nature of the organic phase, and clearly not to a cooling effect because of being in contact with a phase of zero temperature.

The obtained results indicate that the rigid nature of the opposite phase introduces a certain ordering at the water surface. This ordering affects the consecutive subsurface molecular water layers, which become thinner and denser, and get closer to each other, and also the orientation of the surface water molecules. The enhanced orientational ordering at the surface is accompanied by enhanced hydrogen bonding structure, at least within the surface layer, which results in a considerably larger mean residence time of the water

molecules at the surface, i.e., a slower exchange of them between the surface layer and the bulk aqueous phase.

As a consequence of the more ordered layering structure of the water molecules, the global, non-intrinsic density profile of water has turned out to be structured, exhibiting several separate maxima and minima, such as at solid-liquid interfaces formed with an ordered phase [77-82]. This finding contradicts the view that the monotonous non-intrinsic density profiles obtained at the liquid-liquid interface [26-39] are smoothed solely artificially, i.e., by the averaging over the capillary waves in a non-intrinsic treatment, while no such averaging is done (due to the lack of the capillary waves) at the interface with a solid phase of perfectly flat surface. This view is supported by the fact that the real, intrinsic density profiles are structured even at the liquid-liquid interface when, due to the intrinsic treatment, the effect of the capillary waves is removed. [41,42,57,60,61] However, such capillary waves are also present in our "frozen" system, and the obtained non-intrinsic density profile still turned out to be structured. This result clearly reveals that, besides the artificial effect of the non-intrinsic treatment, leading to an erroneous smoothing of the density profiles, the fluid nature of the opposite phase also makes the density profile of the phase of interest smoother (yet still structured), and, unlike the former one, this effect is fully physical and real.

Acknowledgement

This project is supported by the Hungarian OTKA Foundation under project No. 104234.

References

[1] Y. R. Shen, Nature337 (1989) 519.

[2] G. L. Richmond, Chem. Rev. 102 (2002) 2693.

[3] J. Daillant, A. Gibaud, X-Ray and Neutron Reflectivity: Principles and Applications, Springer, Berlin, 1999.

[4] D. Zhang, J. H. Gutow, K. B. Eisenthal, T. F. Heinz, J. Chem. Phys. 98 (1993) 5099.

[5] J. Y. Huang, M. H. Wu, Phys. Rev. E 50 (1994) 3737.

[6] D. E. Gragson, G. L. Richmond, J. Phys. Chem. B 102 (1998) 3847.

[7] D. M. Mitrinović, Z. Zhang, S. M Williams, Z. Huang, M. L. Schlossman, J. Phys. Chem. B 103 (1999) 1779.

[8] X. Zhuang, D. Kim, Y. R. Shen, Phys. Rev. B 59 (1999) 12632.

[9] P. B. Miranda, Y. R. Shen, J. Phys. Chem. B 103 (1999) 3292.

[10] D. Zimdars, J. I. Dadap, K. B. Eisenthal, T. F. Heinz, J. Phys. Chem. B 103 (1999) 3425.

[11] Shi, C.; Anson, F. C. J. Phys. Chem. B 103 (1999) 6283.

[12] C. Fradin, A. Braslau, D. Luzet, D. Smilgies, M. Alba, N. Boudet, K. Mecke, J. Daillant, Nature 403 (2000) 871.

[13] A. L. Barker, P. R. Unwin, J. Phys. Chem. B 104 (2000) 2330.

[14] A. Morita, J. T. Hynes, Chem. Phys. 258 (2000) 371.

[15] L. F. Scatena, M. G. Brown, G. L. Richmond, Science 292 (2001) 908.

[16] E. A. Raymond, T. L. Tarbuck, M. G. Brown, G. L. Richmond, J. Phys. Chem. B 107 (2003) 546.

[17] G. Ma, H. C. Allen, J. Phys. Chem. B 107 (2003) 6343.

[18] Chen, H.; Gan, W.; Lu, R.; Guo, Y.; Wang, H. F. J. Phys. Chem. B 109 (2005) 8064.

[19] G. Luo, S. Malkova, S. V. Pingali, D. G. Schultz, B. Lin, M. Meron, I. Benjamin, P. Vanysek, M. L. Schlossman, J. Phys. Chem. B 110 (2006) 4527.

[20] W. Gan, D. Wu, Z. Zhang, R. Feng, H. Wang, J. Chem. Phys. 124 (2006) 114705.

[21] D. S.Walker, F. G. Moore, G. L. Richmond, J. Phys. Chem. B 111 (2007) 6103.

[22] Y. Fan, X. Chen, L. Yang, P. Cremer, Y. Q. Gao, J. Phys. Chem. B 113 (2009) 11672.

[23] M. J. Shultz, P. Bisson, H. Groenzin, I. Li, J. Chem. Phys. 133 (2010) 054702.

[24] I. V. Stiopkin, C. Weeraman, P. A. Pieniazek, F. Y. Shalhout, J. L. Skinner, A. V. Benderskii, Nature 474 (2011) 192.

[25] M. P. Allen, D. J. Tildesley, Computer Simulation of Liquids, Oxford University Press, Oxford, 1987.

[26] P. Linse, J. Chem. Phys. 86 (1987) 4177.

[27] I. Benjamin, J. Chem. Phys. 97 (1992) 1432.

[28] M. Matsumoto, Y. Takaoka, Y. Kataoka, J. Chem. Phys. 98 (1993) 1464.

[29] Y. Zhang, S. E. Feller, B. R. Brooks, R. W. Pastor, J. Chem. Phys. 103 (1995) 10252.

[30] K. Schweighoffer, I. Benjamin, J. Phys. Chem. 99 (1995) 9974.

[31] M. Tarek, D. J. Tobias, M. L. Klein, J. Chem. Soc. Faraday Trans. 92 (1996) 559.

[32] T. M. Chang, L. X. Dang, J. Chem. Phys. 104 (1996) 6772.

[33] K. Schweighoffer, U. Essmann, M. L. Berkowitz, J. Phys. Chem. B 101 (1997) 3793.

[34] I. Benjamin, J. Chem. Phys. 110 (1999) 8070.

[35] H. Domínguez, M. L. Berkowitz, M. L. J. Phys. Chem. B 104 (2000) 5302.

[36] D. Michael, I. Benjamin, J. Chem. Phys. 114 (2001) 2817.

[37] P. Jungwirth, D. J. Tobias, J. Phys. Chem. B 105 (2001) 10468.

[38] L. X. Dang, J. Chem. Phys. 119 (2003) 6351.

[39] I. Benjamin, J. Phys. Chem. B 109 (2005) 13711.

[40] J. Chowdhary, B. M. Ladanyi, J. Phys. Chem. B 110 (2006) 15442.

[41] M. Jorge, M. N. D. S. Cordeiro, J. Phys. Chem. C 111 (2007) 17612.

[42] M. Jorge, M. N. D. S. Cordeiro, J. Phys. Chem. C 112 (2008) 2415.

[43] L. B. Pártay, G. Horvai, P. Jedlovszky, Phys. Chem. Chem. Phys. 10 (2008) 4754.

[44] L. B. Pártay, P. Jedlovszky, Á. Vincze, G. Horvai, J. Phys. Chem. B 112 (2008) 5428.

[45] L. B. Pártay, P. Jedlovszky, G. Horvai, J. Phys. Chem. C 113 (2009) 18173.

[46] G. Hantal, P. Terleczky, G. Horvai, L. Nyulászi, P. Jedlovszky, J. Phys. Chem. C 113 (2009) 19263.

[47] G. Hantal, M. Darvas, L. B. Pártay, G. Horvai, P. Jedlovszky, J. Phys.: Condens. Matter 22 (2010) 284112.

[48] M. Darvas, K. Pojják, G. Horvai, P. Jedlovszky, J. Chem. Phys. 132 (2010) 134701.
[49] M. Darvas, L. B. Pártay, P. Jedlovszky, G. Horvai, J. Mol. Liq. 153 (2010) 88.
[50] K. Pojják, M. Darvas, G. Horvai, P. Jedlovszky, J. Phys. Chem. C 114 (2010) 12207.
[51] L. B. Pártay, P. Jedlovszky, G. Horvai, J. Phys. Chem. C 114 (2010) 21681.
[52] G. Hantal, M. N. D. S. Cordeiro, M. Jorge, Phys. Chem. Chem. Phys. 13 (2011) 21230.
[53] M. Lísal, Z. Posel, P. Izák, Phys. Chem. Chem. Phys. 14 (2012) 5164.
[54] G. Hantal, I. Voroshylova, M. N. D. S. Cordeiro, M. Jorge, Phys. Chem. Chem. Phys. 14 (2012) 5200.
[55] M. Darvas, G. Horvai, P. Jedlovszky, J. Mol. Liquids 176 (2012) 33.
[56] L. B. Pártay, G. Hantal, P. Jedlovszky, Á. Vincze, G. Horvai, J. Comp. Chem. 29 (2008) 945.
[57] E. Chacón, P. Tarazona, Phys. Rev. Lett. 91 (2003) 166103.
[58] A. P. Wilard, D. Chandler, J. Phys. Chem. B 114 (2010) 1954.
[59] M. Jorge, P. Jedlovszky, M. N. D. S. Cordeiro, J. Phys. Chem. C 114 (2010) 11169.
[60] M. Sega, S. S. Kantorovich, P. Jedlovszky M. Jorge, J. Chem. Phys., 138 (2013) 044110.
[61] M. Jorge, G. Hantal, P. Jedlovszky, M. N. D. S. Cordeiro, J. Phys. Chem. C 114 (2010) 18656.
[62] M. Darvas, M. Jorge, M. N. D. S. Cordeiro, S. S. Kantorovich, M. Sega, P. Jedlovszky, J. Phys. Chem. C, submitted.
[63] M. Darvas, M. Jorge, M. N. D. S. Cordeiro, P. Jedlovszky, J. Mol. Liquids, submitted.
[64] P. Jedlovszky, M. Darvas, G. Horvai, Z. Naturforsch. 68a (2013) 123.
[65] M. Darvas, T. Gilányi, P. Jedlovszky, J. Phys. Chem. B 114 (2010) 10995.
[66] M. Darvas, T. Gilányi, P. Jedlovszky, J. Phys. Chem. B 115 (2011) 933.
[67] N. A. Rideg, M. Darvas, G. Horvai, P. Jedlovszky, J. Phys. Chem. B, submitted.
[68] W. L. Jorgensen, J. Chandrashekar, J. D. Madura, R. Impey and M. L. Klein, J. Chem. Phys. 79 (1983) 926.
[69] E. M. Duffy, D. L. Severance, W. L. Jorgensen, J. Am. Chem. Soc. 114 (1992) 7535.
[70] S. Miyamoto, P. A. Kollman, J. Comp. Chem. 13 (1992) 952.

[71] B. Hess, H. Bekker, H. J. C. Berendsen, J. G. E. M. Fraaije, J. Comp. Chem. 18 (1997) 1463.

[72] U. Essman, L. Perera, M. L. Berkowitz, T. Darden, H. Lee, L. G. Pedersen, J. Chem. Phys. 103 (1995) 8577.

[73] E. Lindahl, B. Hess, D. van der Spoel, J. Mol. Mod. 7 (2001) 306.

[74] S. Nosé, Mol. Phys. 52 (1984) 255.

[75] W. G. Hoover, Phys. Rev. A 31 (1985) 1695.

[76] M. Parinello, A. Rahman, J. Appl. Phys. 52 (1981) 7182.

[77] P. Gallo, M. Rovere, E. Spohr, J. Chem. Phys. 113 (2000) 11324.

[78] I. Brovchenko, A. Geiger, A. Oleinikova, J. Phys.: Condens. Matter 16 (2004) S5345.

[79] M. Předota, A. V. Bandura, P. T. Cummings, J. D. Kubicki, D. J. Wesolowski, A. A. Chialvo, M. L. Machesky, J. Phys. Chem. B 108 (2004) 12049.

[80] P. Jedlovszky, M. Předota, I. Nezbeda Mol. Phys. 104 (2006) 2465.

[81] G. Nagy, M. C. Gordillo, E. Guardia, J. Marti, J. Phys. Chem. B 111 (2007) 12524.

[82] E. Tombácz, A. Hajdú, E. Illés, K. László, G. Garberoglio, P. Jedlovszky, Langmuir 25 (2009) 13007.

[83] J. Chowdhary, B. M. Ladanyi, Phys. Rev. E 77 (2008) 031609.

[84] P. Jedlovszky, Á. Vincze, G. Horvai, J. Chem. Phys. 117 (2002) 2271.

[85] P. Jedlovszky, Á. Vincze, G. Horvai, Phys. Chem. Chem. Phys. 6 (2004) 1874.

[86] D. Stauffer, Introduction to percolation theory, Taylor and Francis, London, 1985.

Tables

Table 1. Properties of the first three molecular layers of the aqueous phase in the two systems simulated.

system	layer	density profiles		surface roughness		dynamics of exchange
		X_c/Å	σ/Å	a/Å	ξ	τ/ps
I (frozen)	first	22.00	2.88	1.73	0.98	13.3
	second	19.01	2.94	1.66	0.97	
	third	16.12	3.11	1.70	1.06	
II (reference)	first	22.07	3.77	2.34	0.93	6.6
	second	18.96	3.71	2.27	0.84	
	third	15.97	3.71	2.25	0.84	

Figure caption

Fig. 1. Left: instantaneous equilibrium snapshots of the “frozen” system I (top) and the “reference” system II. Water O and H atoms are shown by red and white, whilst the atoms of the CCl_4 molecules by grey balls, respectively. Right: water molecules constituting the first three molecular layers of the aqueous phase in these systems. Molecules of the first, second and third layer are marked by green, brown and purple colours, respectively.

Fig. 2. Mass density profile of water in systems I (“frozen”, red dashed line) and II (“reference”, black solid line) along the macroscopic interface normal axis *X*. The density profiles corresponding to the first three molecular layers of water in systems I (orange open circles) and II (blue full circles) are also shown, together with the Gaussian functions fitted to these data (system I: orange dashed lines, system II: blue solid lines). The inset illustrates the division of the surface molecular layer of water into the three separate regions A, B and C (see the text). All profiles shown are averaged over the two interfaces present in the basic simulation box.

Fig. 3. Roughness curves (i.e., average normal distance of two surface points as a function of their lateral distance, see the text) of the first three molecular layers in systems I (red open symbols) and II (black full symbols). The curves corresponding to the first, second and third layers are shown by circles, squares and triangles, respectively. The lines correspond to the functions fitted to these data according to Eq. (1).

Fig. 4. Survival probability of the water molecules in the surface molecular layer of systems I (red open symbols) and II (black full symbols). The exponentially decaying functions fitted to these data are shown by solid lines.

Fig. 5. Orientational maps of the water molecules in the entire surface layer (top row) as well as in its separate regions A (second row), B (third row) and C (bottom row) of systems I (left column) and II (right column). Lighter colours correspond to higher probabilities.

Fig. 6. Size distribution of the lateral hydrogen bonded clusters in the first (circles) and second (squares) molecular layer of the aqueous phase in systems I (red open symbols) and II (black full symbols). The critical line of percolation corresponding to Eq. (2) is also shown by a solid line. For better visibility, the data are shown on a double logarithmic scale.

Figure 1.

Kertész et al.

system I (frozen)

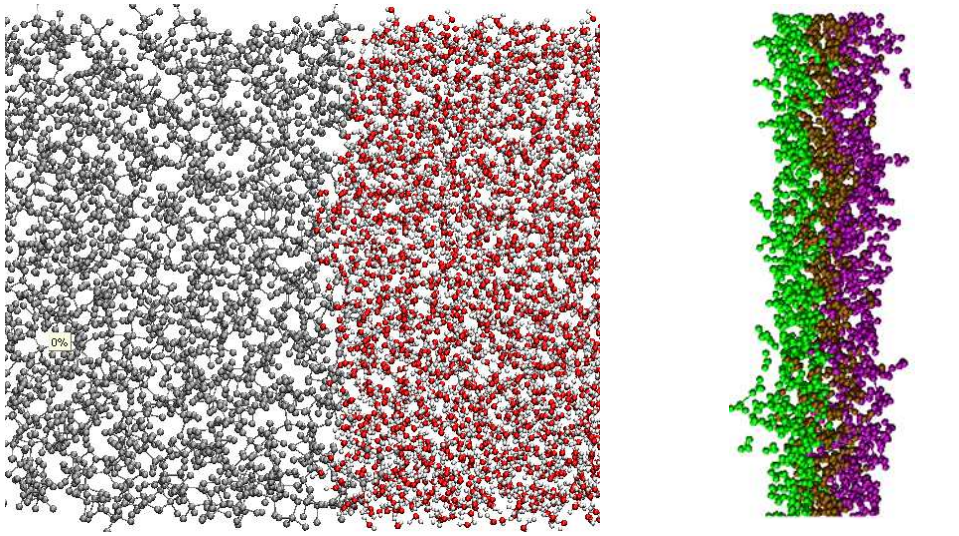

system II (reference)

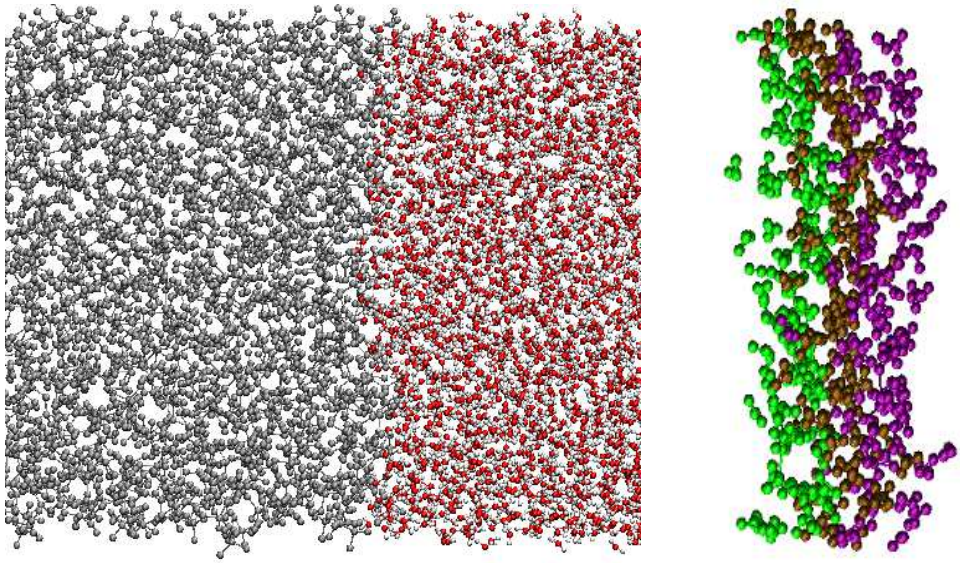

Figure 2.

Kertész et al.

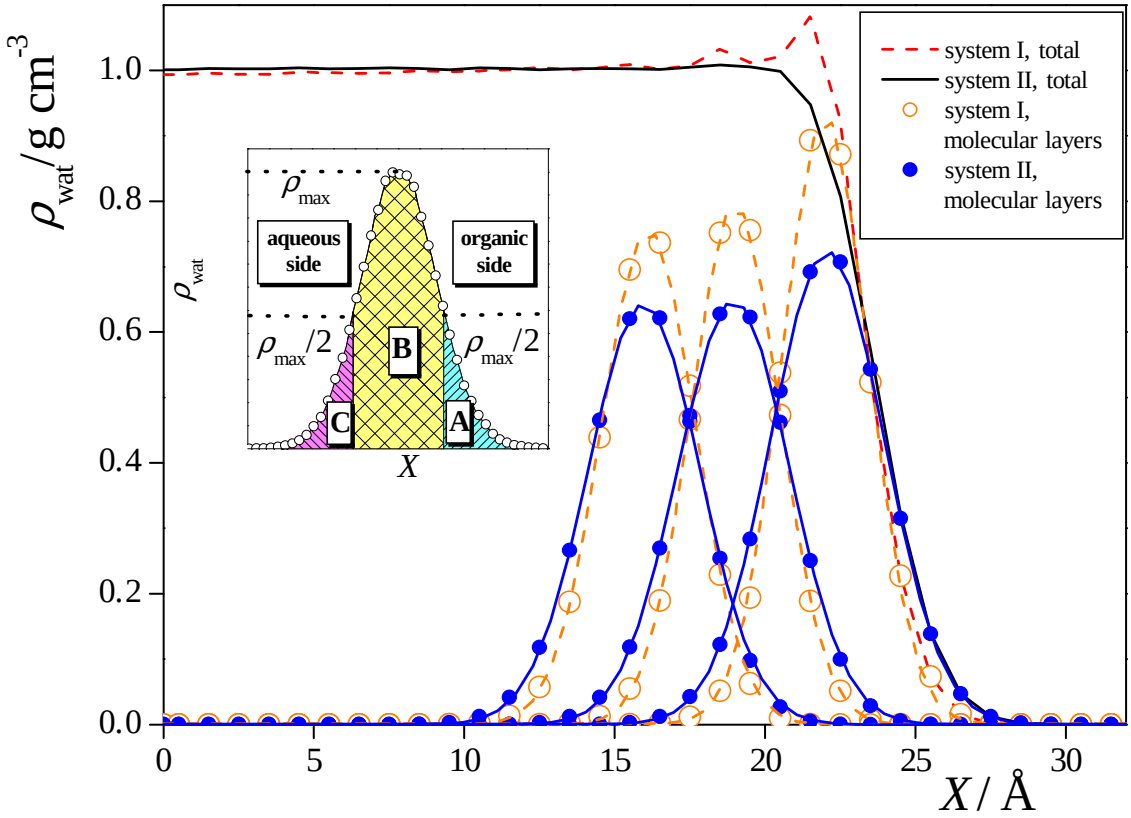

Figure 3.

Kertész et al.

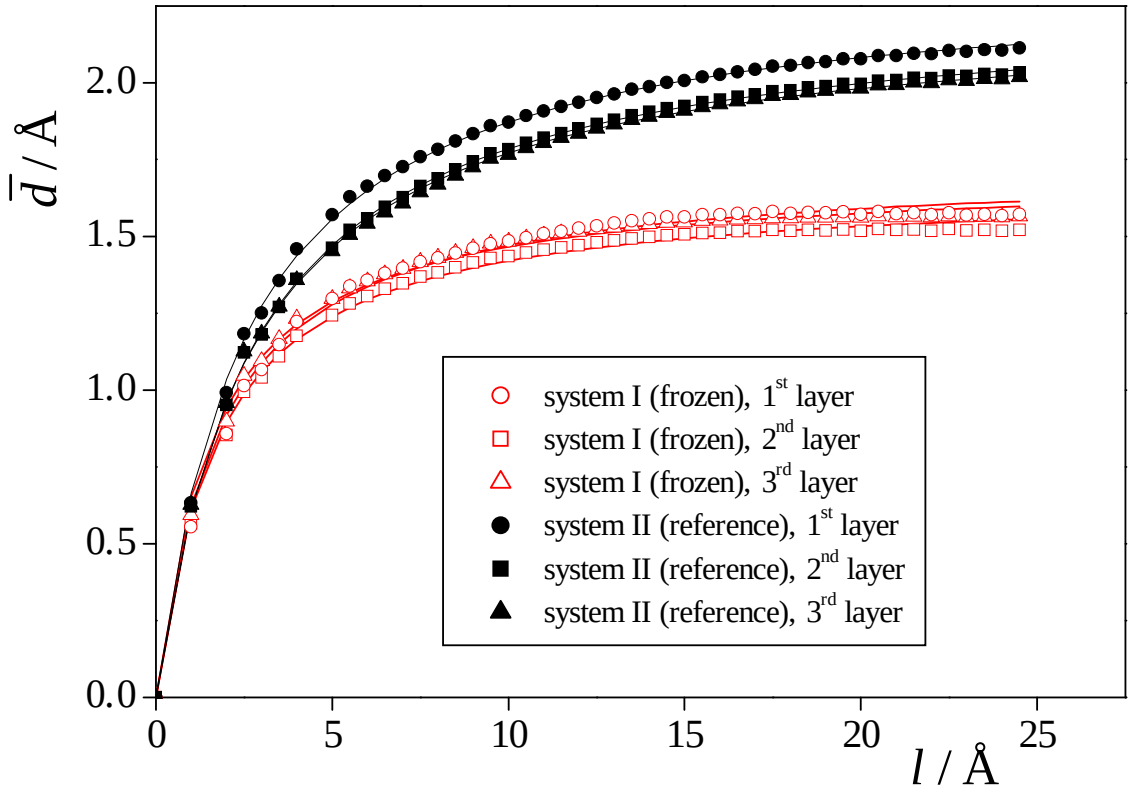

Figure 4.

Kertész et al.

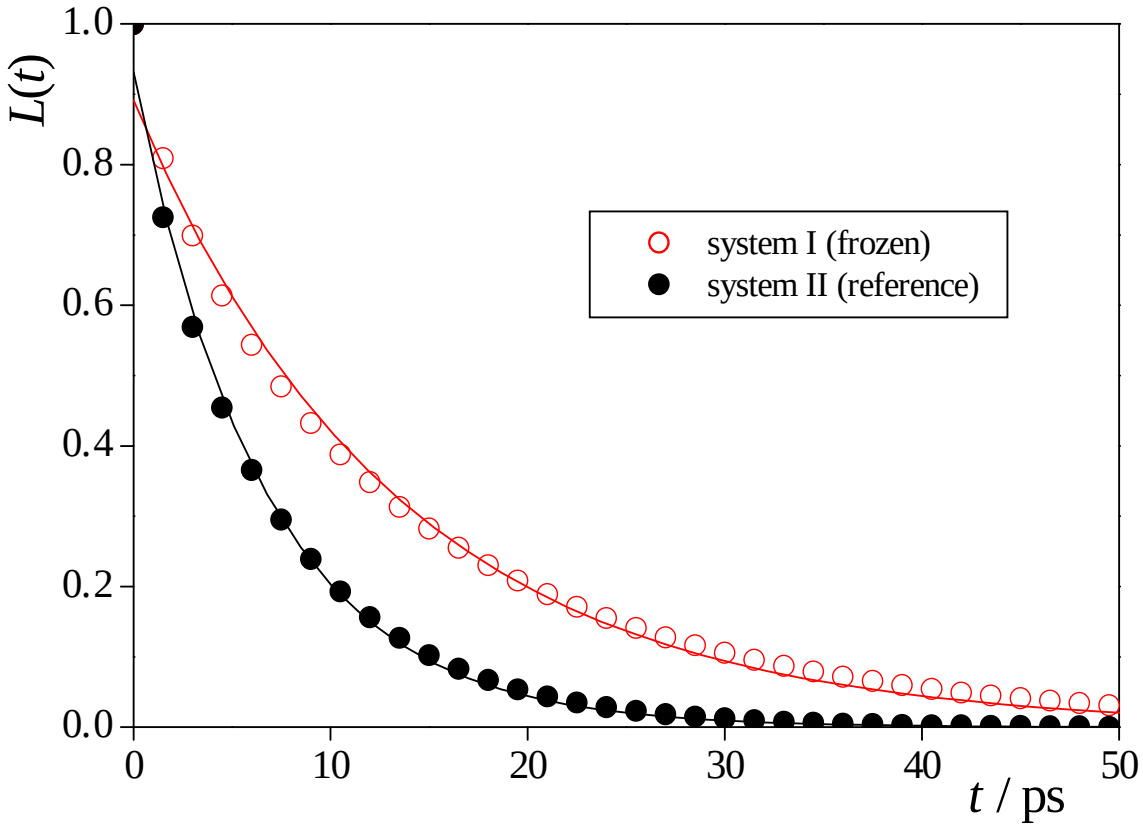

Figure 5.

Kertész et al.

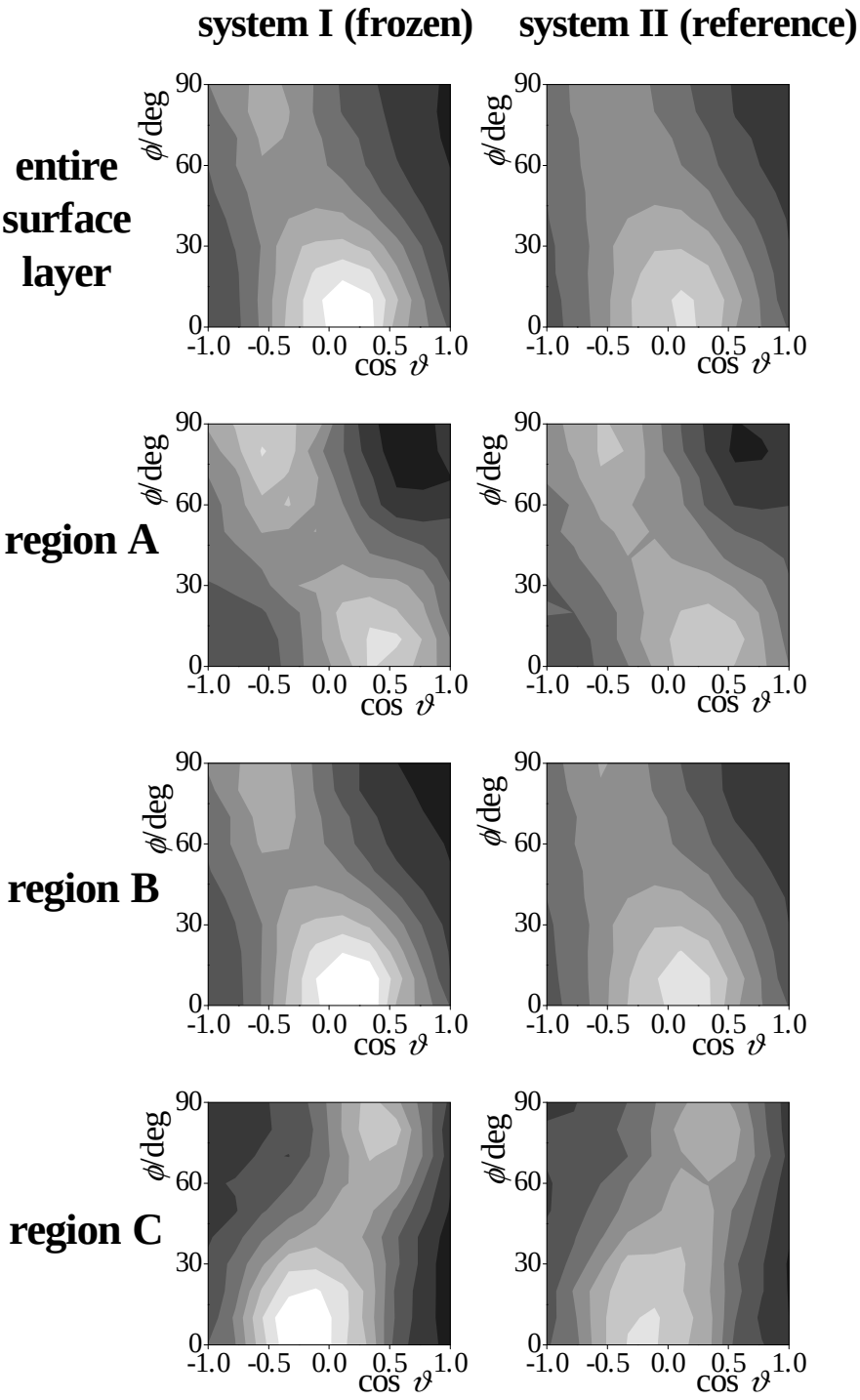

Figure 6.

Kertész et al.